Supplementary Information

Supplementary Table 1. HDAC inhibitors tested with healthy donor PBMCs and their biochemical potency (nM) across HDACs 1, 2, 3, and 6.

	HDAC1	HDAC2	HDAC3	HDAC6	Reference
Entinostat	125	340	370	>50000	Witter DJ, Bioorg. Med. Chem. Lett., 2008
Ricolinostat	58	48	51	5	Santo L, Blood, 2012
ACY-241	35	45	46	2	Pengyu Huang, Oncotarget, 2017
ACY-738	94	128	218	2	Jochems J, Neuropsychopharmacology, 2014
ACY-775	2,123	2,570	11,223	8	Jochems J, Neuropsychopharmacology, 2014
Tubastatin A	3,259	3,575	4,948	19	Jochems J, Neuropsychopharmacology, 2014

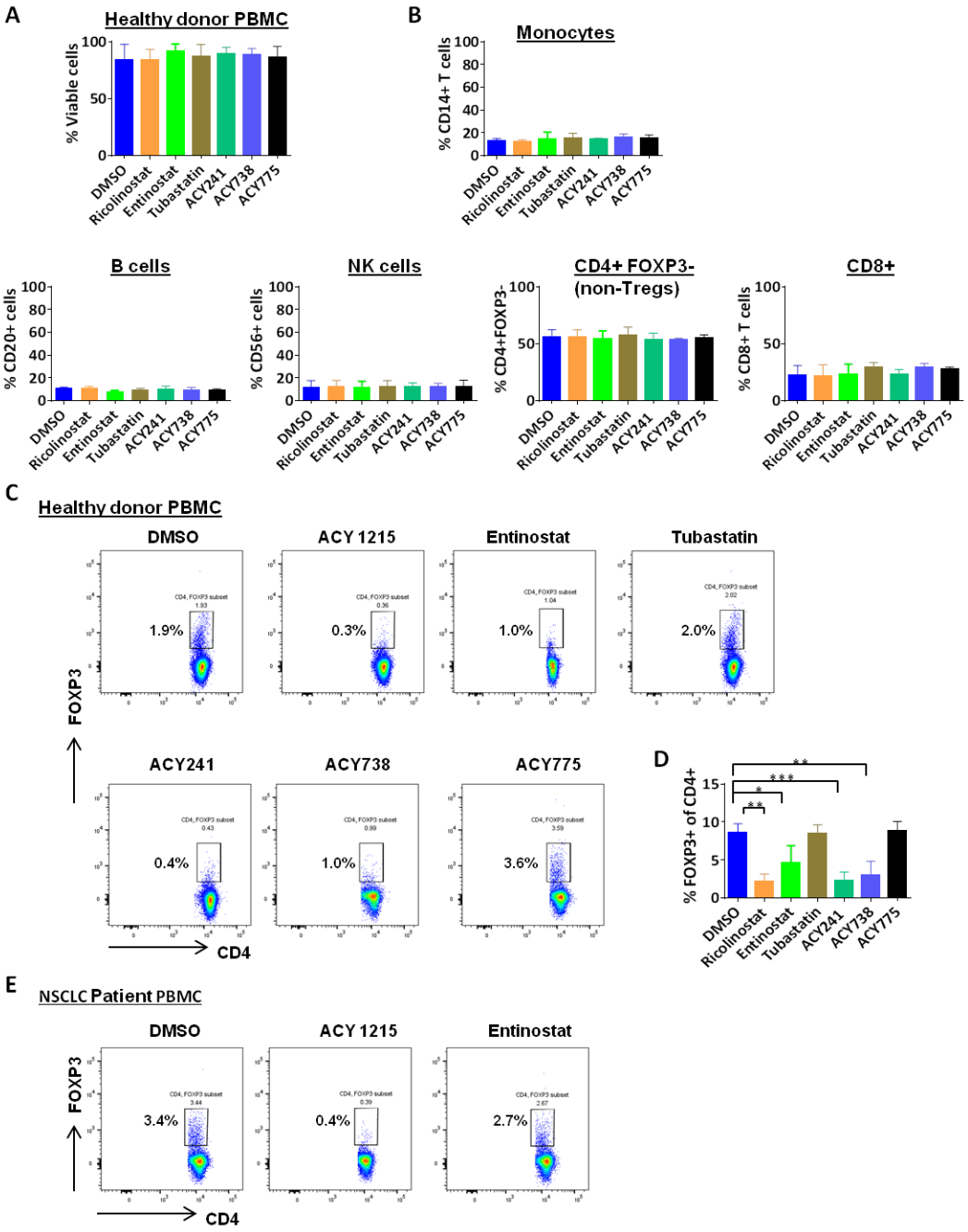

Supplementary Figure 1. Reduced CD4+FOXP3+ Treg cells in healthy donor and NSCLC patient PBMC in the presence of ricolinostat.

Peripheral blood mononuclear cells (PBMC) from healthy donors (A-D) or NSCLC patients (E) were cultured with 2.5μm of indicated HDAC inhibitors (described in table 1) for 24 hours after

which the frequency of T cell subsets was assessed by FACS. DMSO was used as a control. (A) Percent of live cells as determined by fraction of total cells that were negative for the live/dead viability dye. (B) Percent of monocytes, B, NK, CD4+FOXP3- and CD8+ T cells in total viable PBMC after culture with indicated HDAC inhibitors. (C, E) Representative dot plots and (D) summary of proportions of CD4+Foxp3+ Treg cells after 24-hour culture of (C, D) healthy donor or (E) NSCLC patient PBMC with indicated drugs. Data represent the mean ±SEM of samples analyzed from 5-8 subjects. * indicates p-value < 0.05, ** indicates p-value <0.01, *** indicates p-value <0.001.

Supplementary Table 2. Information for consented Non-small cell lung cancer (NSCLC) patients that underwent surgical resectioning as part of their treatment plan and whose tumor specimen and blood samples obtained after surgery were analyzed.

Patient ID	Age	Sex	Smoking history	Histology
2502	69	Male	Smoker	Adenocarcicoma
83671	64	Male	Smoker	Adenosquamous
49385	67	Female	Non-smoker	Adenocarcinoma
58863	75	Male	Non-smoker	Adenocarcinoma
45542	59	Male	Smoker	Squamous

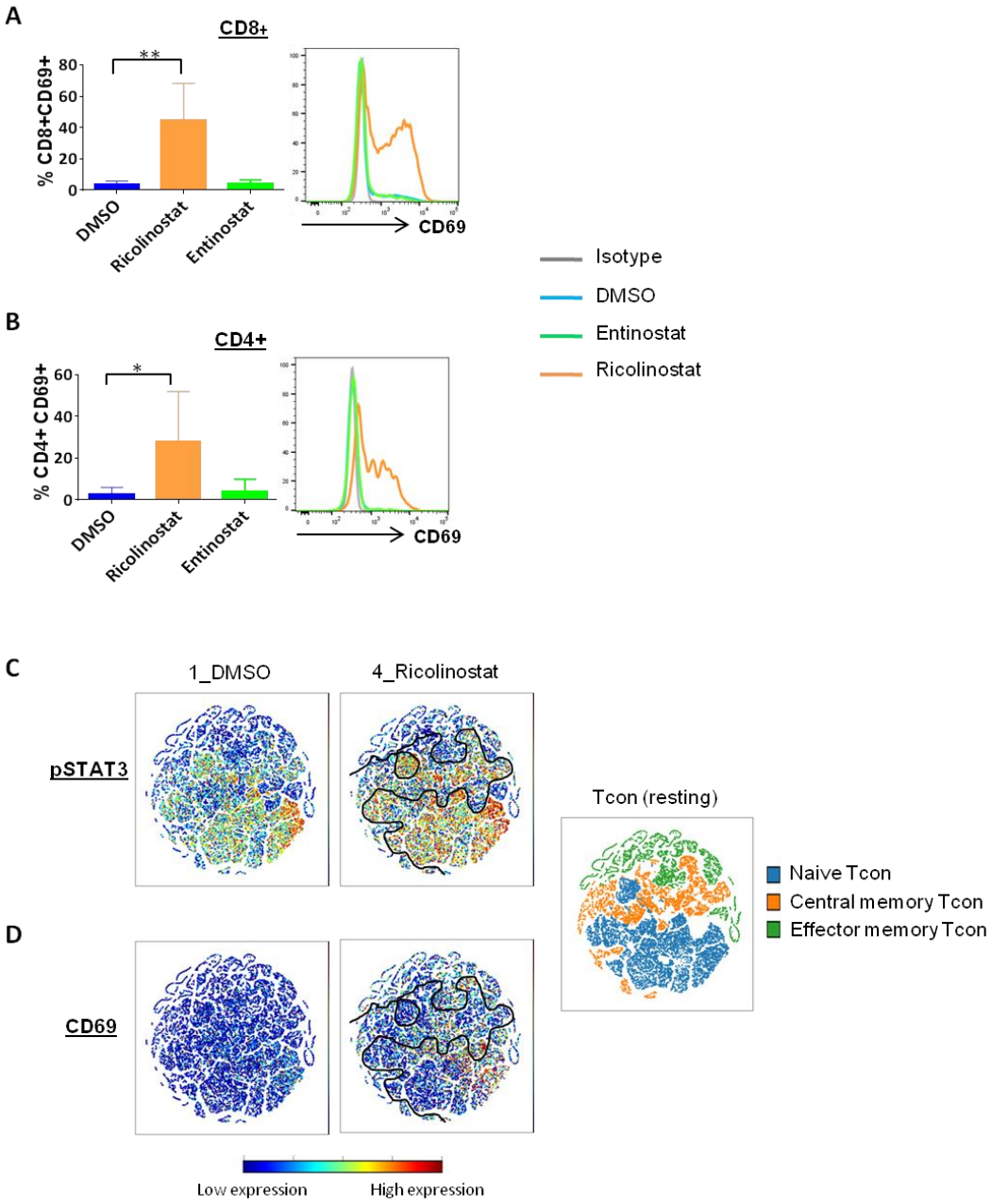

Supplementary Figure 2. Up-regulation of CD69 on T cells in healthy donor PBMC cultures in the presence of ricolinostat.

Peripheral blood mononuclear cells (PBMC) from healthy donors were cultured with ricolinostat or entinostat for 24 hours after which the phenotype of T cell subsets was assessed by FACS. DMSO was used as a control. Summary (left) and representative histograms (right) for

expression levels of CD69 on gated (A) CD8+ and (B) CD4+ T cells within the PBMC cultures. The phenotype of PBMCs cultured as above was further evaluated by CyTOF analysis. Representative profiles for (C) phospho-STAT3 or (D) CD69 expression on depicted CD3+ T conventional (Tcon) cell subsets after total T cell culture with indicated agents. Data represent the mean ±SEM of samples analyzed from 8 healthy donors (A, B) or one representative of five independent experiments analyzed from 5 healthy donors(C, D). * indicates p-value < 0.05, ** indicates p-value <0.01.

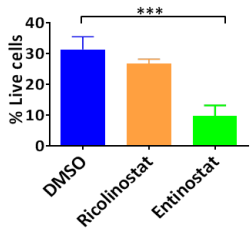

Supplementary Figure 3. Viability of immune cells within dissociated tumor specimens cultured in the presence of ricolinostat or entinostat. Tumor specimens obtained from consented NSCLC patients were de-bulked by gentle dissociation following incubation with DNAse and collagenase. Cells were then cultured with 2.5 µm of ricolinostat or entinostat for 3 days. Percent of live cells as determined by fraction of total leukocytes that were negative for the live/dead viability dye. Data represent the mean ±SEM of 5 independent experiments.

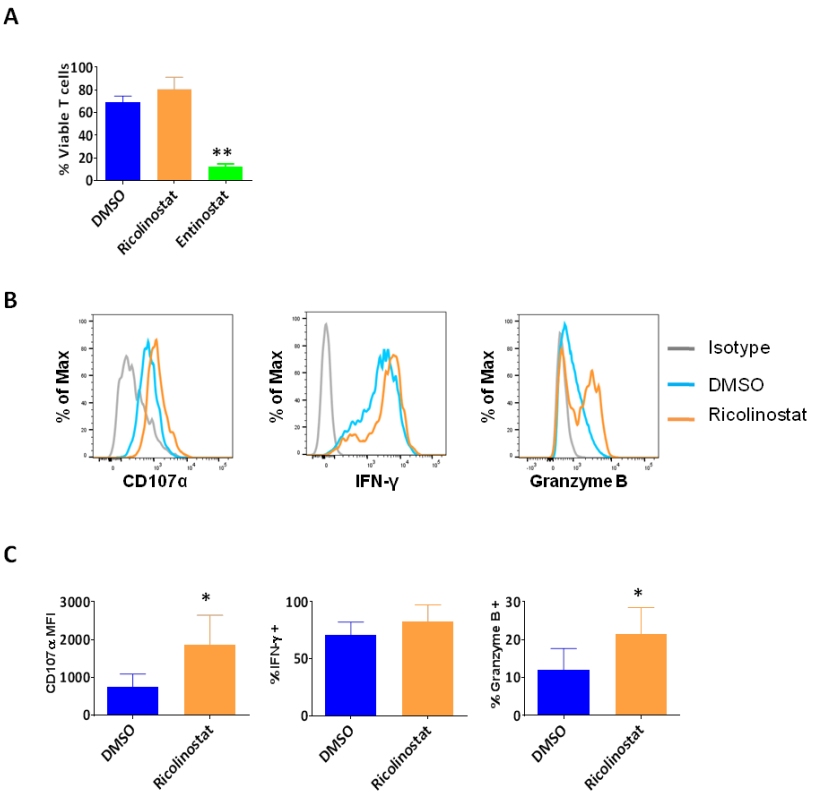

Supplementary Figure 4. Effector function of T cells within 2-D cultures of disaggregated tumor specimens from NSCLC patients.

Tumor specimens obtained from consented NSCLC patients were de-bulked by gentle dissociation following incubation with DNAse and collagenase. Cells were then cultured with 2.5 µm of ricolinostat or entinostat in the presence of 20IU recombinant IL-2 for 3 days. (A) Percent of live cells as determined by fraction of total CD45+ leukocytes that were negative for live/dead viability dye. Patient tumor cultures were washed and re-stimulated with PMA+ionomycin in the presence of golgi plug for 6 hours. (B) Representative histograms and (C) summary for the expression (MFI) of CD107α (left), percent of IFN-γ positive (middle) and granzyme B+ (right) CD3+CD8+ T cells as assessed by intracellular cytokine staining. Data represent the mean ±SEM of samples analyzed from 5 patients. Entinostat cultures not done due to low viability. * indicates p-value < 0.05, ** indicates p-value <0.01.

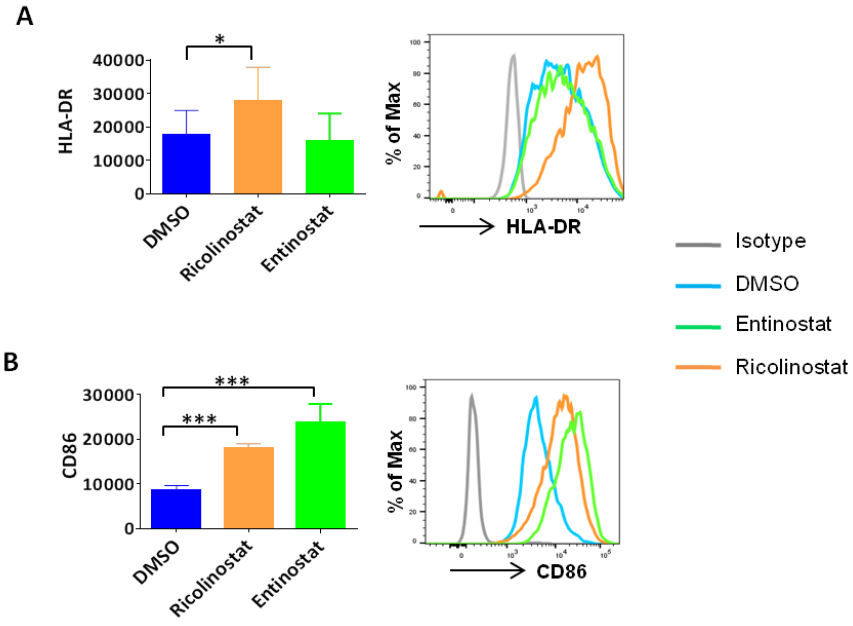

Supplementary Figure 5. Increased expression of MHC class II and CD86 on monocytes in healthy donor PBMC in the presence of ricolinostat.

Peripheral blood mononuclear cells (PBMC) from healthy donors were cultured with ricolinostat or entinostat for 24 hours after which the phenotype of CD3-CD14+ monocytes was assessed by

FACS. DMSO was used as a control. Summary (left) and representative histograms (right) for expression levels of (A) HLA-DR (MHC class II) and (B) co-stimulatory molecule CD86 on gated CD3-CD14+ monocytes. Data represent the mean ±SEM of samples analyzed from 6-8 subjects. * indicates p-value < 0.05, *** indicates p-value <0.001.

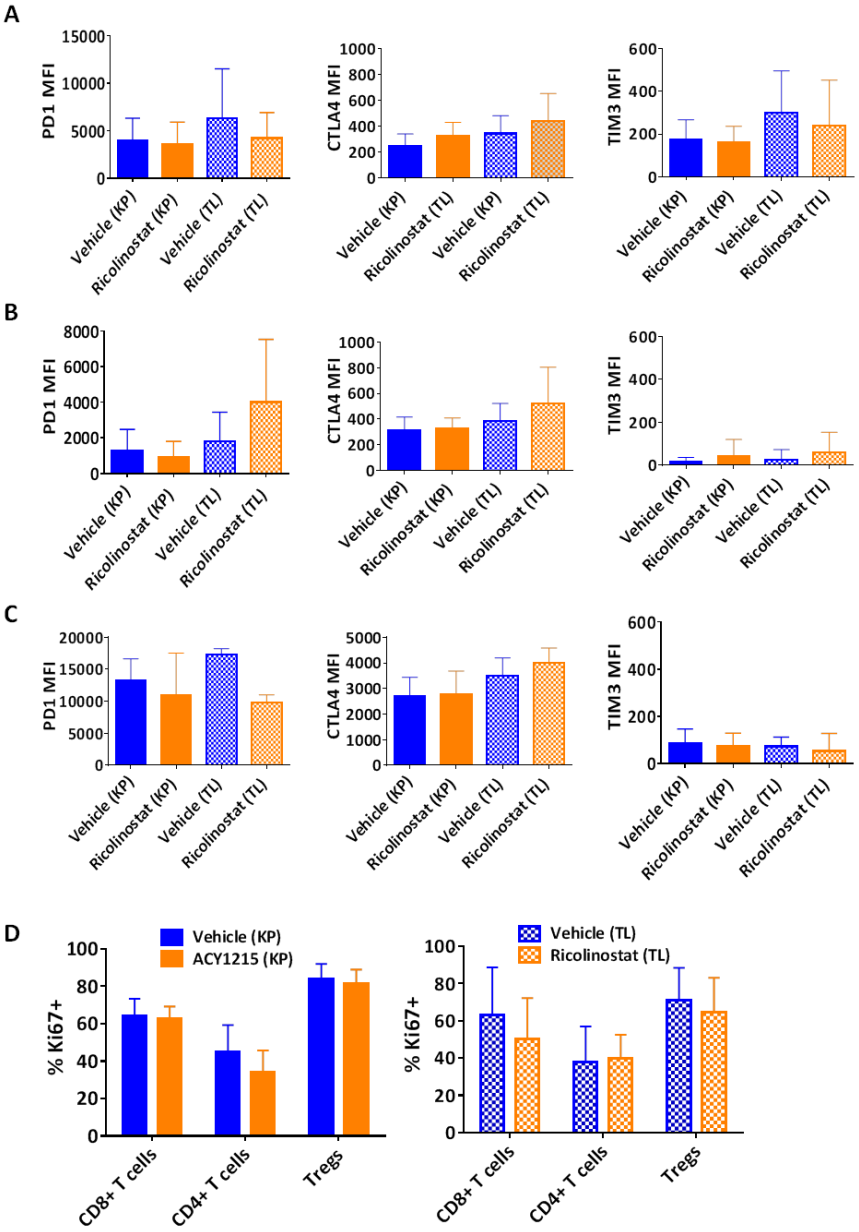

Supplementary Figure 6. Phenotype of T cells infiltrating lung tumors of genetically engineered mice treated with ricolinostat.

Lung tumors (as confirmed by MRI) that spontaneously developed in KP or TL mice upon intranasal delivery of adenovirus-cre recombinase were excised after a 7-day treatment with ricolinostat or vehicle as control. Single cell suspensions were generated and subjected to FACS analysis to assess the phenotype of CD45+ immune cell subsets within the tumors. (A-C) Expression levels of PD-1 (left), CTLA-4 (middle), and TIM3 (right) on tumor-infiltrating (A) CD3+CD8+, (B), CD3+CD4+Foxp3-, and (C) CD3+CD4+Foxp3+ T cells in both KP and TL mice under indicated treatments. (D) Percent of indicated T cell subsets expressing Ki67 in tumors of KP (left) or TL (right) mice under each treatment. Data are mean ±SEM of 5-9 mice per group.

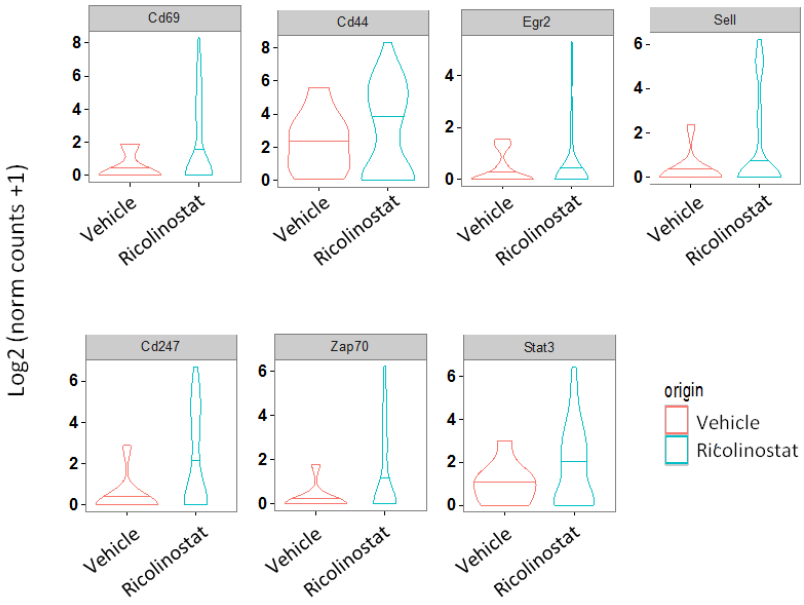

Supplementary Figure 7. Gene expression profile of Tumor-infiltrating T cells.

Tumor nodules excised from lung tumor-bearing KP mice were excised after two-week treatment with ricolinostat or vehicle as control. Single cell suspensions generated from pooled tumor nodules were stained for markers identifying conventional T cells (EpCam-CD45+CD3+CD25dim/-). Single cells were then sorted into individual wells of a 96-well plate after which they were subjected to RNA-Seq. Shown is gene expression profile of cells sorted from tumors of vehicle versus ricolinostat-treated mice.

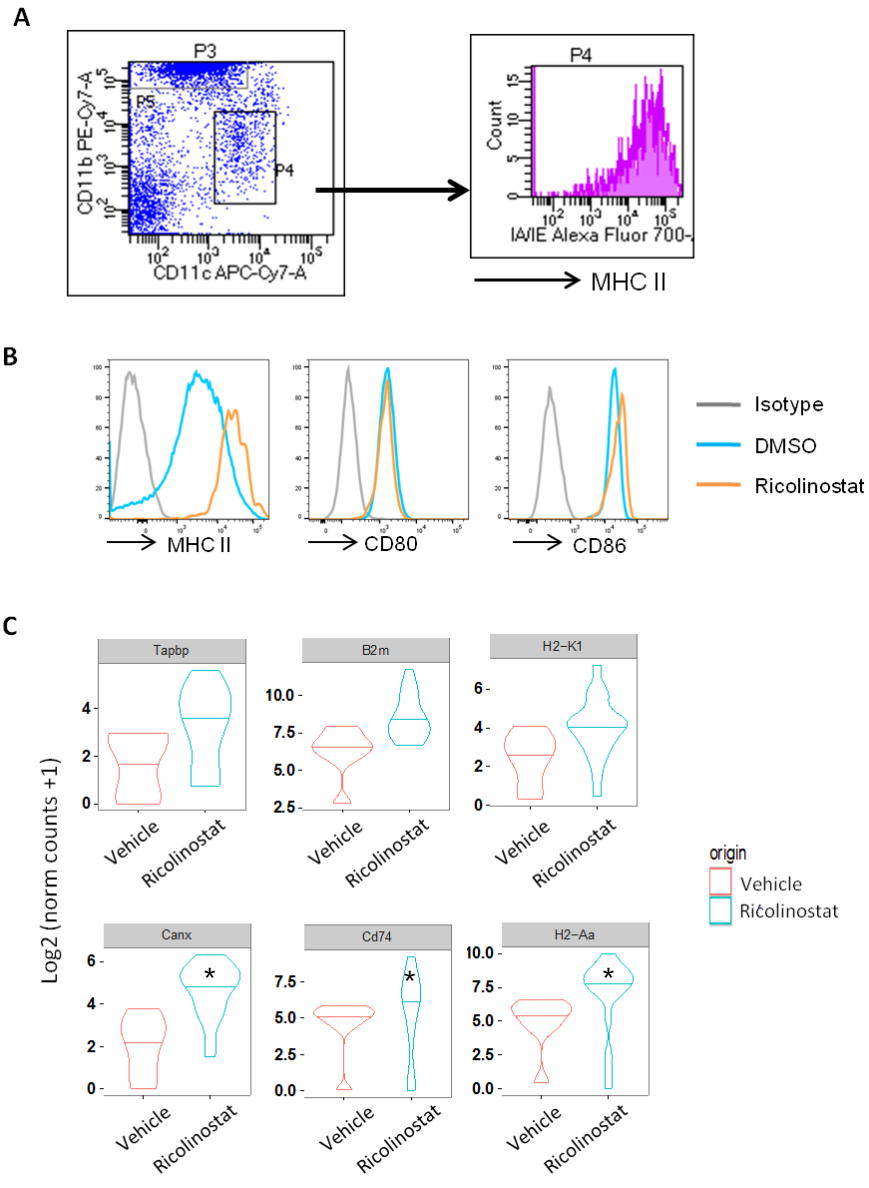

Supplementary Figure 8. Ricolinostat promotes up-regulation of MHC class II and CD86 on tumor-associated macrophages.

(A) Gating strategy for CD111b^{lo}CD11c+ tumor-associated macrophages (TAMs) in the GEM mice as described in fig 3 (left) with corresponding representative histogram plot (right) for MHC class II expression. (B) Representative histogram plots for the expression levels of MHC class II, CD80, and CD86 in TAMs of KP mice treated as indicated. Single cell suspensions generated from pooled tumor nodules as described in SFig.7 were stained for markers identifying TAMs (EpCam-CD45+CD11b^{lo}CD11c+). Single cells were then sorted into individual wells of a 96-well plate after which they were subjected to RNA-Seq. (C) Shown is gene expression profile of TAMs sorted from tumors of vehicle versus ricolinostat-treated mice. * indicates p-value < 0.05.

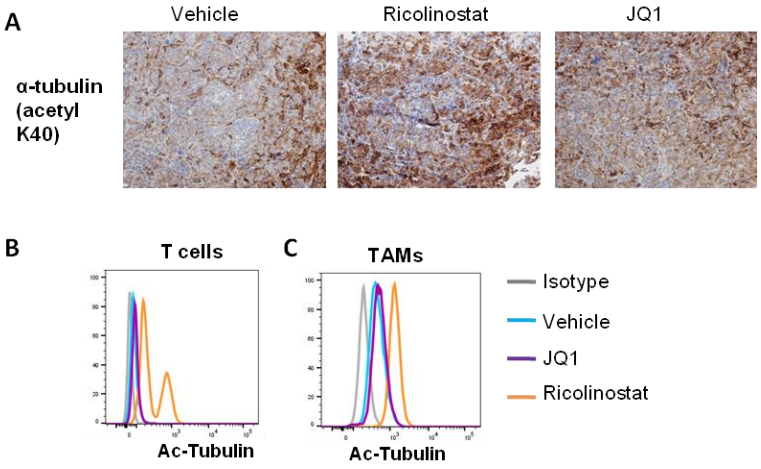

Supplementary figure 9. Immunohistochemical and flow cytometric analyses of acetylated α-tubulin in lung tumors of KP mice.

(A). Expression of alpha tubulin (acetyl K40) in formalin fixed, paraffin embedded tumor sections from KP mice treated with vehicle or ricolinostat as assessed by immunohistochemistry, or by (B, C) FACS analysis of fresh tumor cell suspensions after gating on (B) T cells or (C) tumor-associated macrophages (TAMs). Data from mice treated with JQ1 is included for reference.

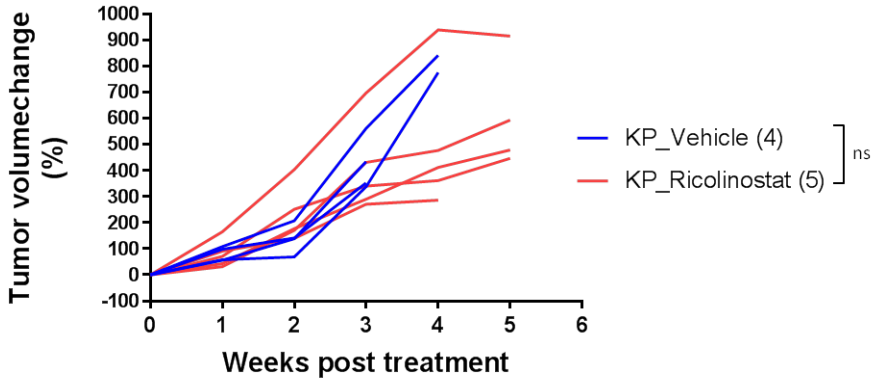

Supplementary Figure 10. Kinetics of tumor growth in KP mice treated with ricolinostat.

KP mice with starting tumor burdens of approximately 200 mm^3 were intraperitoneally injected once daily for 5-6 weeks with ricolinostat and tumor growth was monitored weekly by MRI. Percent change in tumor volume was calculated based on tumor growth relative to the starting tumor size. ns; not significant.

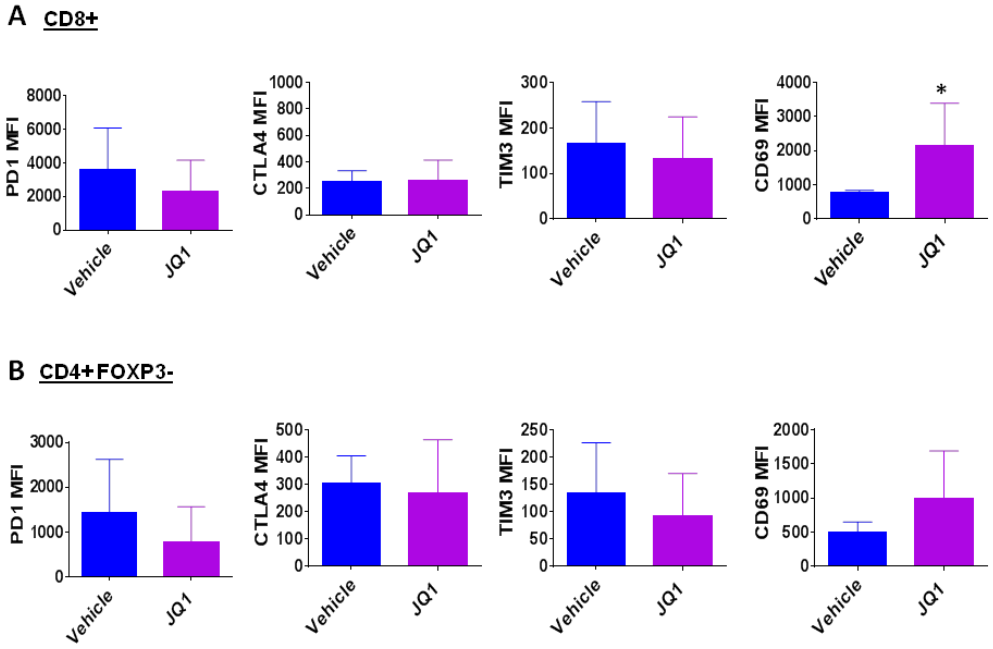

Supplementary Figure 11. Phenotype of tumor-infiltrating T cell subsets in lung tumors of

KP mice treated with JQ1.

Single cell suspensions were generated from lung tumor nodules excised from KP mice that were treated with JQ1 for 1 week and subjected to FACS analysis. Mice that received vehicle served as controls. Summary of expression levels of PD-1, CTLA-4, TIM-3, and CD69 on tumor-infiltrating (A) CD8+ or (B) CD4+ Foxp3- T cells. Data are mean ±SEM of 5-6 mice per group. * indicates p-value < 0.05.

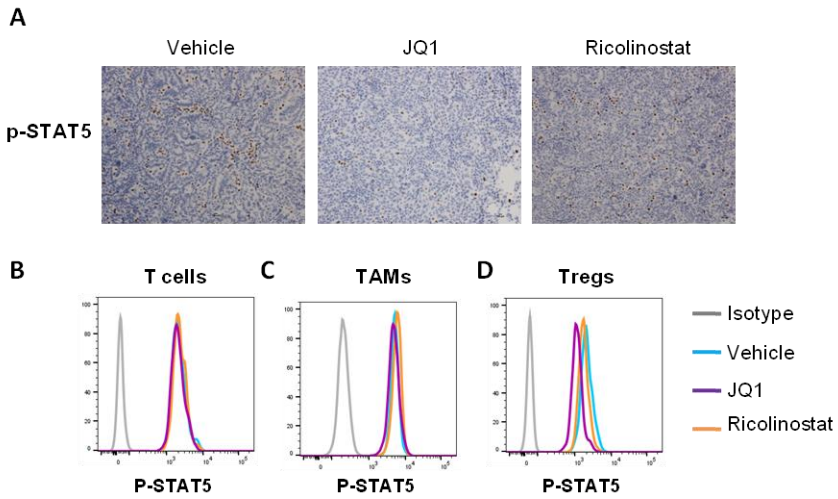

Supplementary Figure 12. Immunohistochemical and flow cytometric analyses of phospho-STAT5 levels in lung tumors of KP mice. (A). Expression of phospho-STAT5 (Tyr694) in formalin fixed, paraffin embedded tumor sections from KP mice treated with vehicle or JQ1 as assessed by immunohistochemistry, or (B-D) FACS analysis of fresh tumor cell suspensions after gating on (B) T cells, (C) tumor-associated macrophages (TAMs), and (D) Tregs. Data from mice treated with ricolinostat is included for reference.

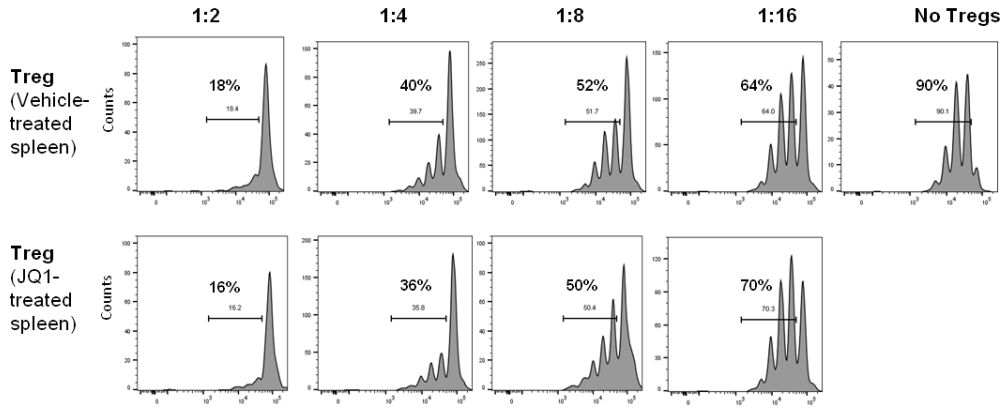

Supplementary Figure 13. Suppressive function of Tregs isolated from the spleen of lung tumor-bearing KP mice treated with JQ1.

CD4+CD25hi Treg cells were sorted from the spleen of vehicle or JQ1-treated KP mice and co-cultured with CFSE-labeled splenic CD4+CD25- T cells ($0.5x10^5$) isolated from the same mouse. Cells were stimulated with α-CD3 (0.25μg/ml) in the presence of T-depleted splenocytes as APCs ($0.25x10^5$) for 3 days. Representative CFSE profiles of proliferating T cells in the presence of Tregs at indicated Treg: T cell ratios. Data is representative of 4 independent experiments.

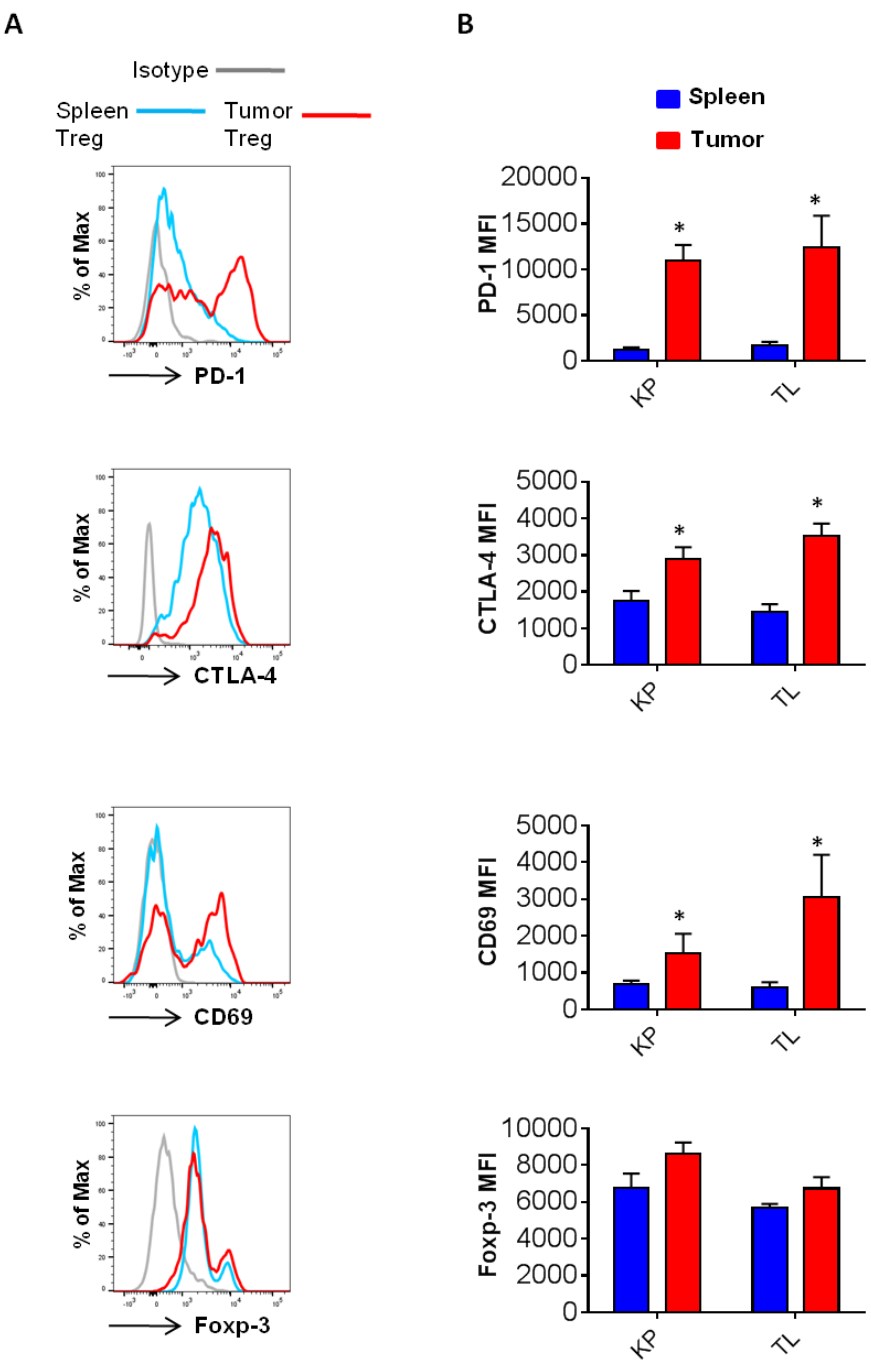

Supplementary Figure 14. Phenotype of Tregs in the spleen or lung tumors of genetically engineered mouse models (GEMM) of NSCLC.

Single cell suspensions generated from lung tumor nodules excised from untreated KP and TL mice were subjected to FACS analysis. (A) Representative histograms and (B) Summary of expression levels for PD-1, CTLA-4, CD69 and Foxp3 on splenic or tumor-infiltrating CD4+Foxp3+ Treg cells in indicated GEMM. Data in (B) are mean ±SEM of 5-6 mice per group. * indicates p-value < 0.05.

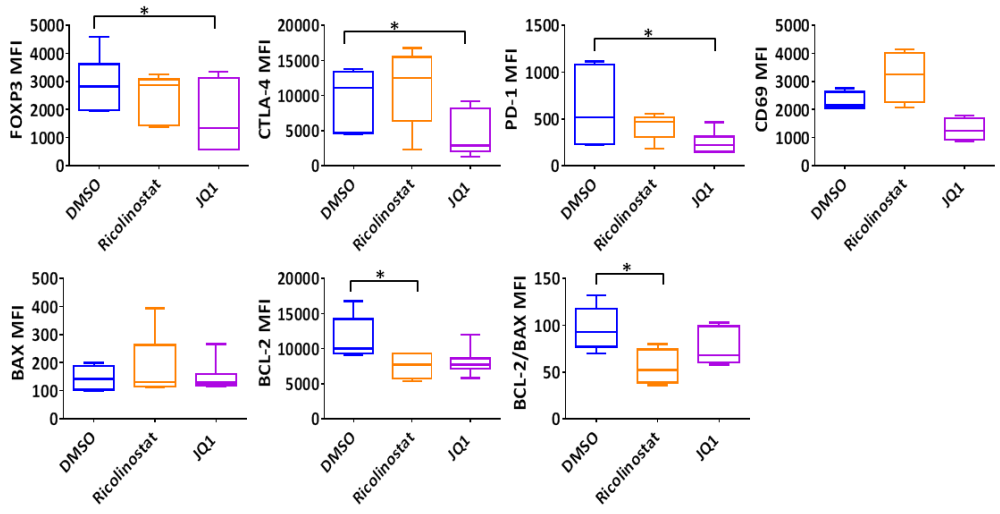

Supplementary Figure 15. Phenotype of Tregs within cultures of dissociated tumor specimen from NSCLC patients.

Surgically re-sected tumor specimen from NSCLC patients were dissociated into cell suspensions and cultured for 48 hours with ricolinostat or JQ1 supplemented with 100IU of recombinant human IL-2 after which the phenotype of the Treg subset was assessed by FACS. DMSO was used as a control. Summary of expression levels for indicated protein molecules on gated CD4+FOXP3+ T cells within the tumor cultures based on mean fluorescent intensity (MFI). Data represent the mean ±SEM of samples analyzed from 5 patients. * indicates p-value < 0.05.

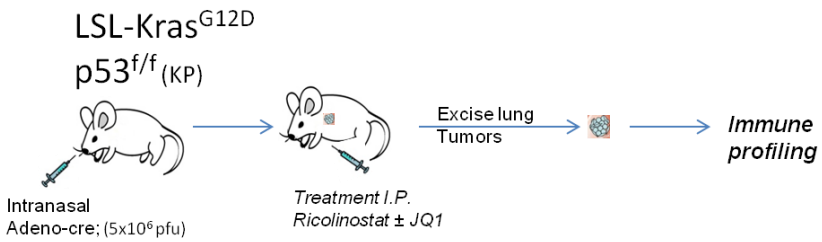

Supplementary Figure 16. In vivo treatment studies. Schematics of in vivo treatment studies in KP mice. Lung tumor-bearing KP mice as confirmed by MRI following intranasal adenovirus-cre recombinase delivery were administered intraperitoneally (I.P.) with ricolinostat and/or JQ1. Mice were treated for 4-6 weeks prior to immune-phenotyping of tumor cell suspensions or assessment of tumor burden in individual mice. Mice that received vehicle served as controls.

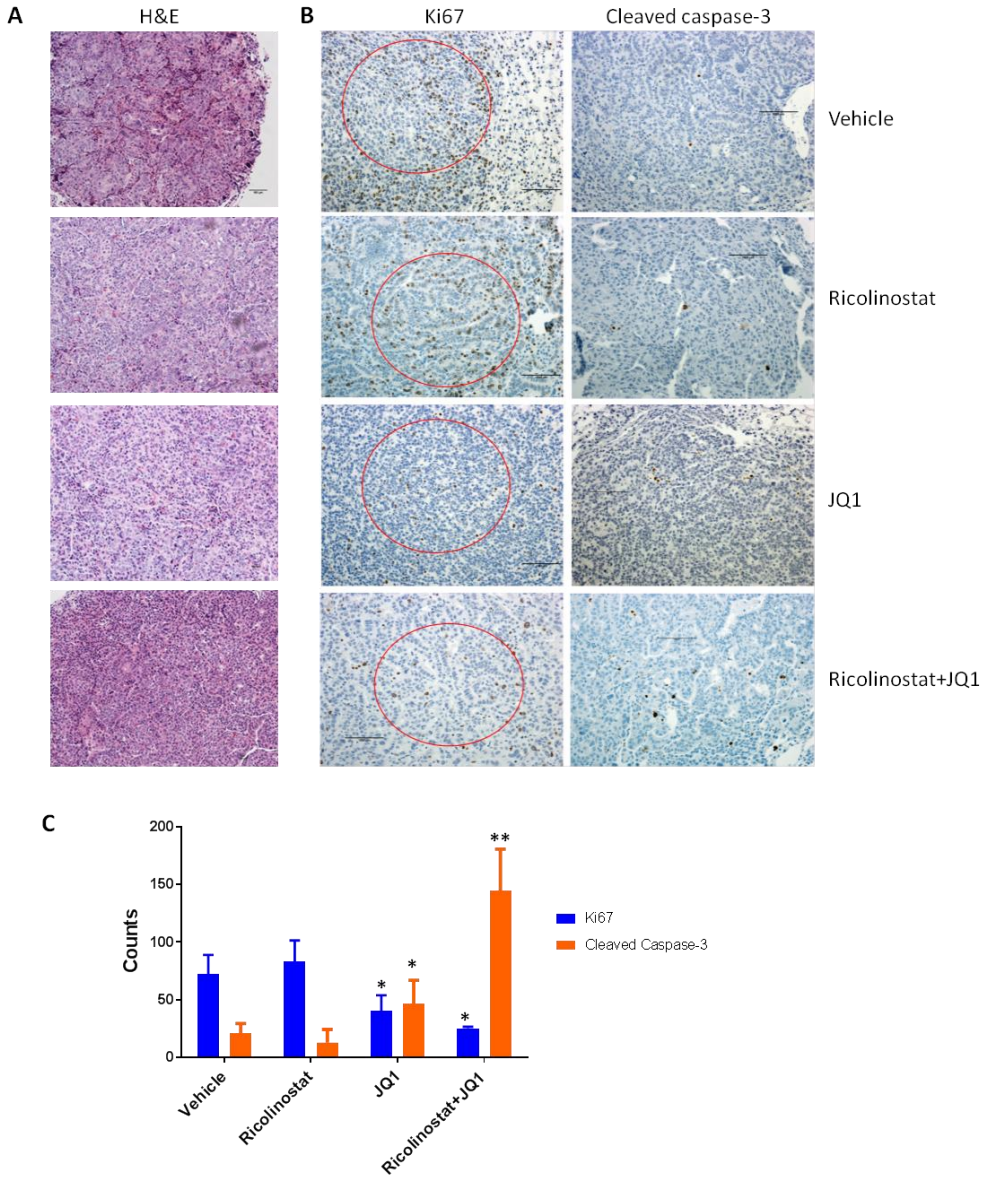

Supplementary Figure 17. Histology and immunohistochemical staining of lung tumor sections from treated KP mice. KP mice were treated with vehicle or ricolinostat and/or JQ1 for 4-

6 weeks after which formalin-fixed, paraffin embedded sections generated from tumor nodules were stained and analyzed. A). Hematoxylin and eosin stain. Magnification; x20. (B) Representative immunohistochemical stain showing expression of Ki67 and cleaved Caspase-3 in the tumor sections. (Representative areas are circled in red for Caspase-3). Scale bars represent 100 μm for all panels. (C) Plots of average Ki67 and cleaved Caspase-3-positive cells in five selected tumor areas of each slide. * indicates p-value < 0.05, ** indicates p-value <0.01.

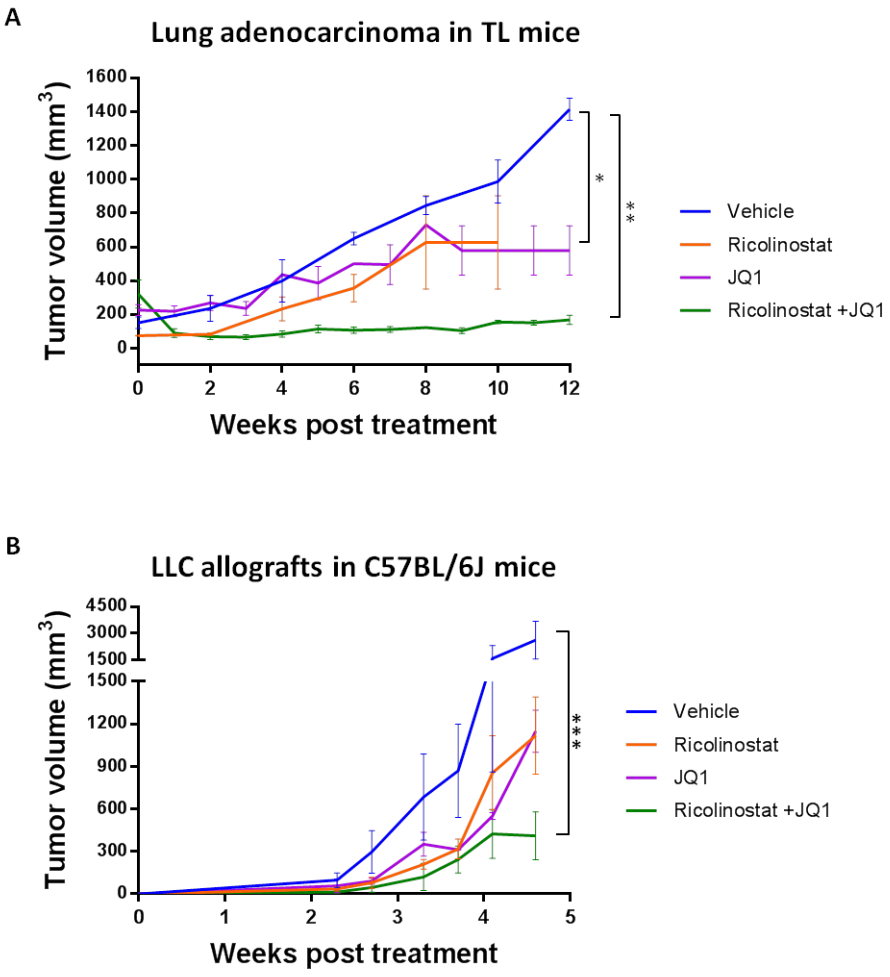

Supplementary Figure 18. Kinetics of tumor growth in TL or wild-type mice.

(A) TL mice with tumor burdens of approximately 200 mm^3 were intraperitoneally injected once daily with ricolinostat and JQ1, and tumor growth was monitored for up to 12 weeks. (B) 500,000 Lewis lung carcinoma cells were implanted into C57BL/6 (B6) mice. Three days after implantation, mice were randomly assigned to groups of 5 for vehicle, JQ1 and/or ricolinostat treatment. Tumors were

measured twice per week and tumor volume was calculated as 0.5*L*W*W. Data represent mean ± SEM of 5 mice per group.

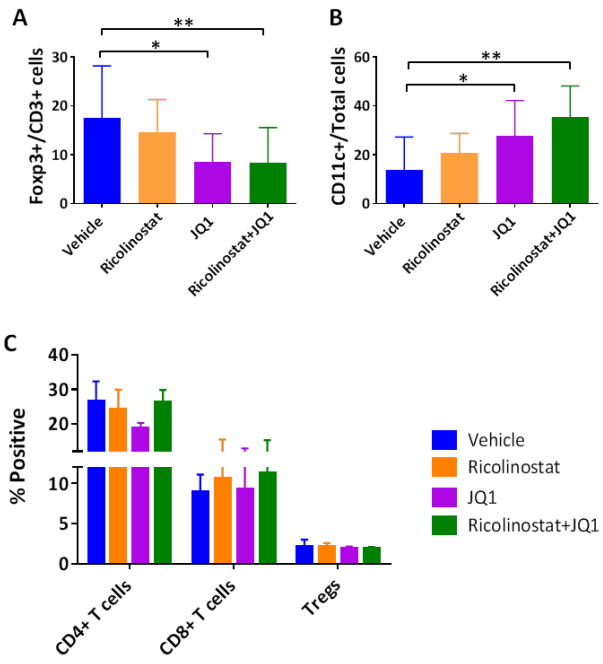

Supplementary Figure 19. Quantification of T cell subsets and TAMs in tumors of KP mice.

Cell suspensions generated from tumor nodules of KP mice that were treated with vehicle, ricolinostat and/or JQ1 for 4-6 weeks were subjected to immunofluorescent staining (A-B) or FACS (C) to determine the proportions of tumor immune cell subsets. (A) Proportion of Tregs (Foxp3+) as a fraction of T cells, and (B) TAMs (CD11c+) within tumor sections from indicated groups of treated mice. Quantification of positive signals for indicated cell types was determined from an average of 10-11 fields of view as evaluated by fluorescent microscopy. (C) Summary of CD4+, CD8+, and Tregs (CD4+Foxp3+) populations in the spleen of these mice. * indicates p-value < 0.05, ** indicates p-value <0.01.

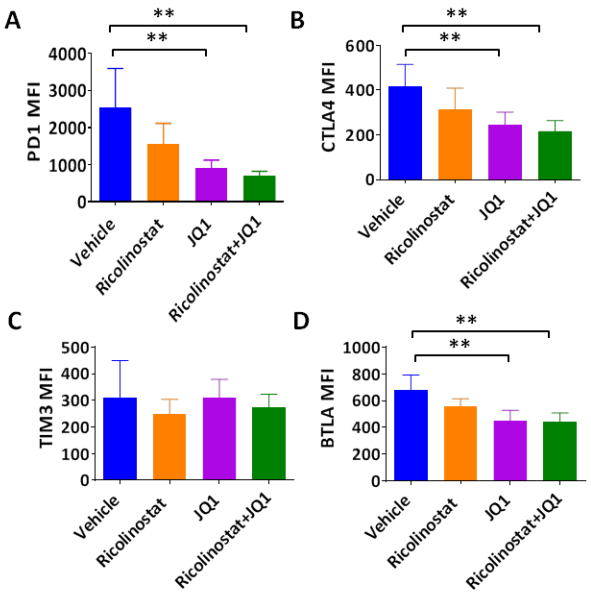

Supplementary Figure 20. Phenotype of CD8+T cells infiltrating lung tumors of treated KP mice.

Tumor nodules were excised from the lungs of KP mice after 5-6 week treatment with vehicle, ricolinostat and/or JQ1. Single cell suspensions were generated and subjected to FACS analysis to assess the phenotype of T cells in the tumors. Expression levels (MFI) of (A) PD-1, (B) CTLA-4, (B) TIM3, and (D) BTLA on gated tumor-infiltrating CD45+CD3+CD8+ T cells. Data are mean ±SEM of 5-6 mice per group. ** indicates p-value <0.01.

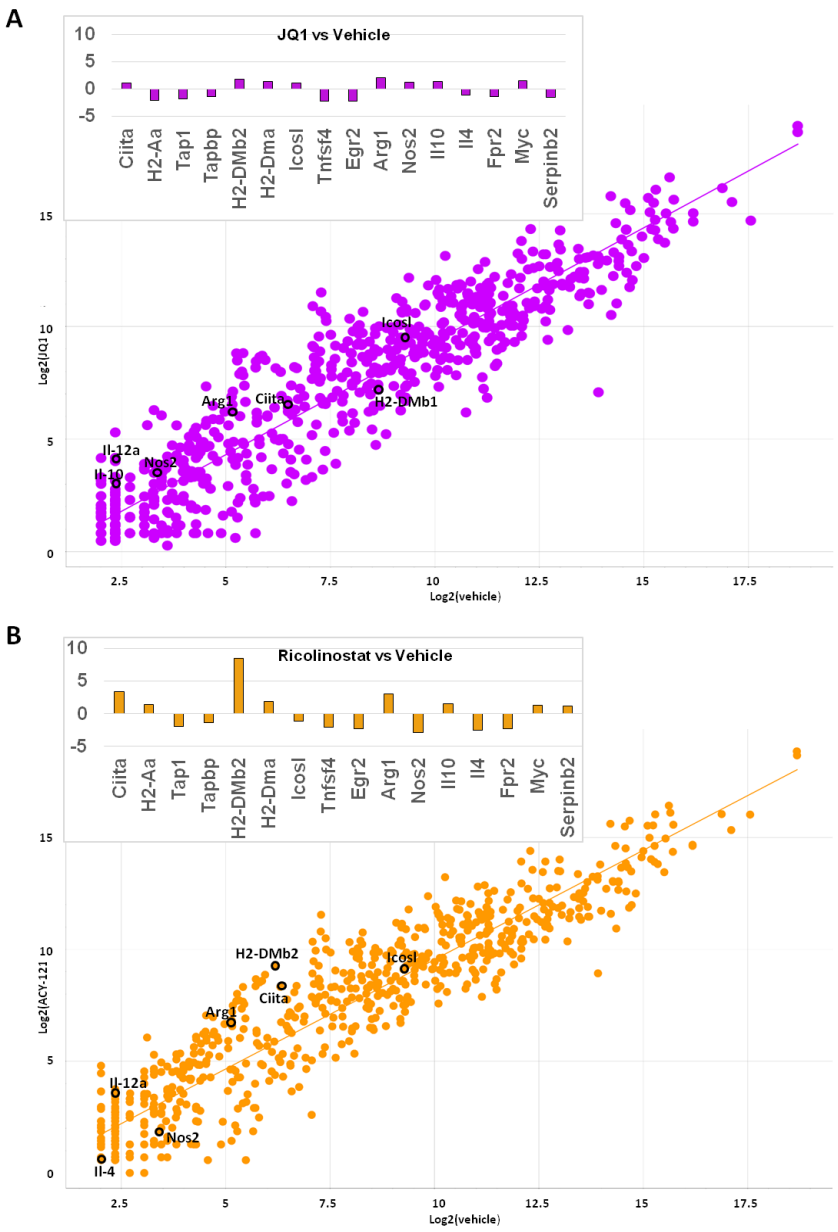

Supplementary Figure 21. Gene expression profile of tumor-infiltrating macrophages (TAMs) in treated KP mice.

Tumor nodules were excised from the lungs of tumor-bearing KP mice after 7-10-day treatment with JQ1, ricolinostat (ACY1215), or vehicle as control. Single cell suspensions were generated from pooled tumor nodules after which TAMs were isolated by AutoMACS following incubation with CD11c microbeads. Total RNA was subsequently isolated from each cell populations and subjected to gene expression profiling using the nanostring platform for gene transcript analysis. Gene expression profile of TAMs isolated from the tumors of (A) JQ1 or (B) ricolinostat-treated KP mice relative to equivalent cells from vehicle group expressed as fold change of select indicated genes (top) or log2 counts (bottom). Highlighted on the scatter plots are also some of the genes depicted in the graphs.

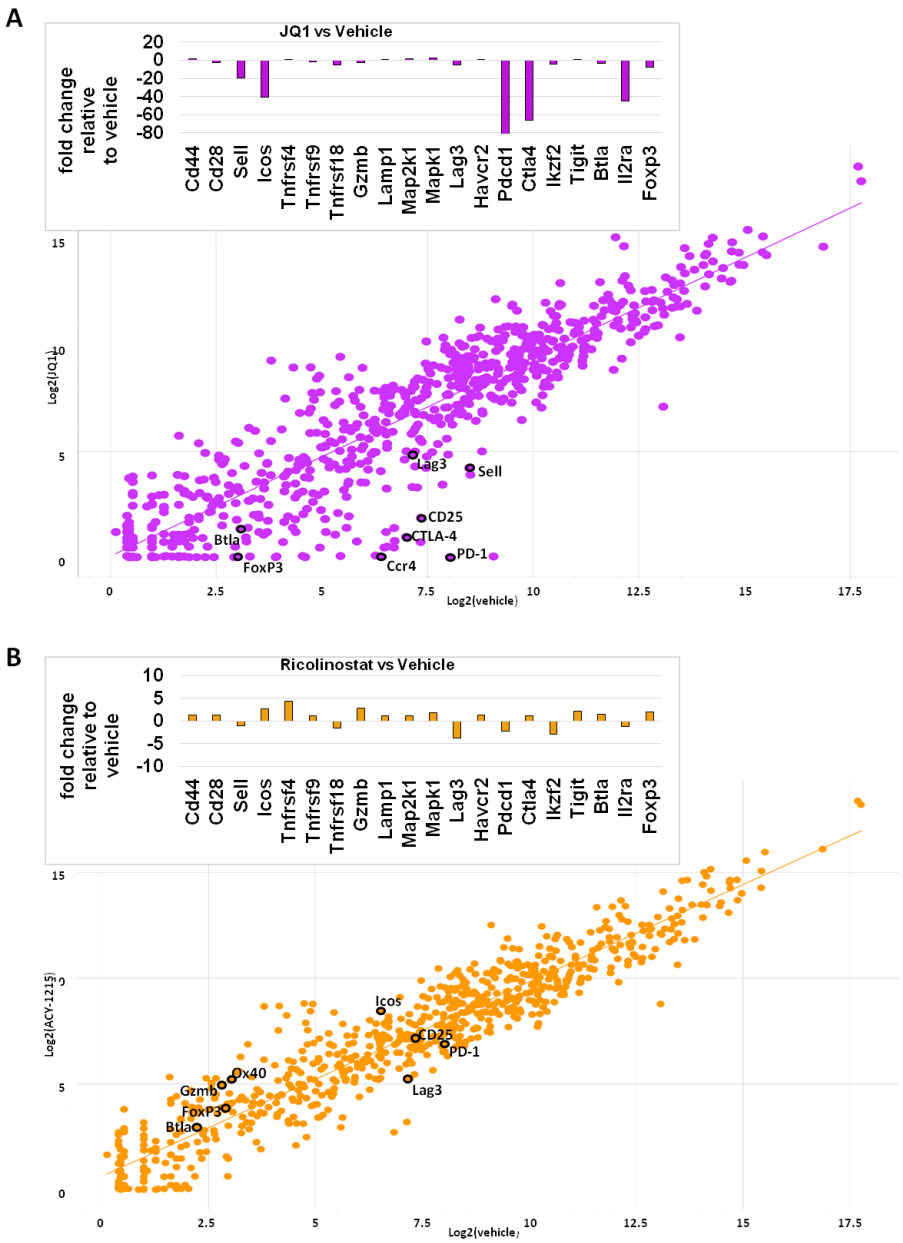

Supplementary Figure 22. Gene expression profile of tumor-infiltrating macrophages T cells in treated KP mice. Tumor nodules were excised from the lungs of tumor-bearing KP mice after 7-10-day treatment with JQ1, ricolinostat (ACY1215) or vehicle as control. Single cell suspensions were generated from pooled tumor nodules after which T cells were isolated by AutoMACS following incubation with CD90.2 microbeads. Total RNA was subsequently isolated from each cell populations and subjected to gene expression profiling using the nanostring platform for gene transcript analysis. Gene expression profile of T cells isolated from the tumors of (A) JQ1 or (B) ricolinostat-treated KP mice relative to equivalent cells from vehicle group expressed as fold change of select indicated genes (top) or log2 counts (bottom). Highlighted on the scatter plots are also some of the genes depicted in the graphs.

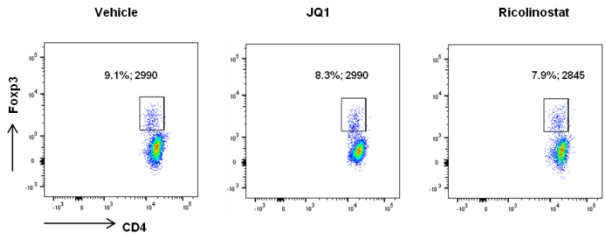

Supplementary Figure 23. Proportion of CD4+Foxp3+ Tregs present within tumor-infiltrating T cells utilized in gene expression studies.

Representative dot plots of proportions of CD4+Foxp3+ Treg cells within CD4+ T cell fraction in mice treated as indicated, and from which T cells wer e purified for nanostring. Data is representative of 3-4 mice/group.

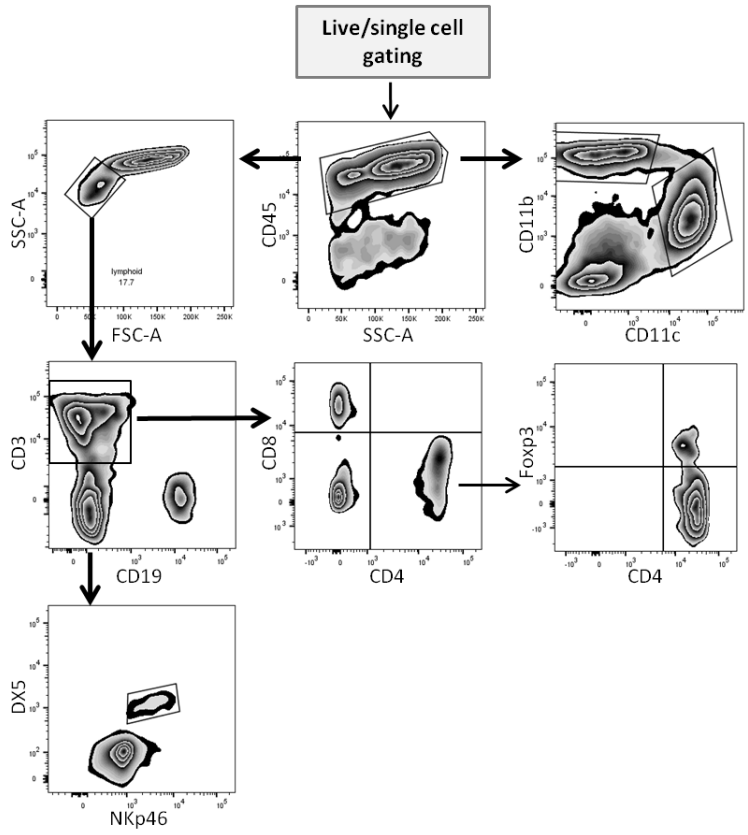

Supplementary Figure 24. Gating strategy.

Gating strategy employed for identification of viable CD45+ leukocyte subsets in mouse tumor cell suspensions analyzed by FACS.

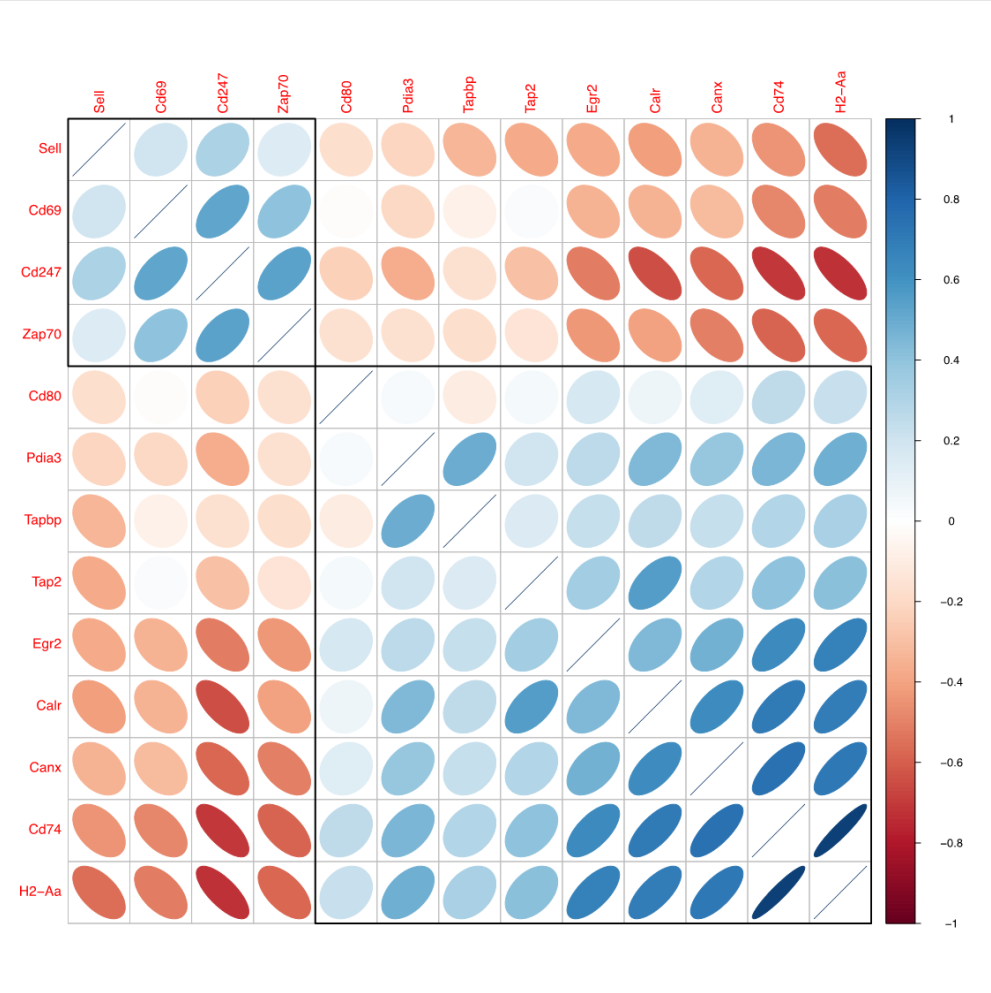

Supplementary Figure 25. Correlation plot for the expression of indicated genes in CD45+ leukocytes in KP tumors as evaluated by single cell RNA-Sequencing.

Shown are the relative expression levels and their correlation pattern for genes of interest as described in supplementary figure 7 and 8C.

Supplementary Methods

Antibodies

The following antibodies were utilized for FACS analyses of PBMCs and patient tumor studies: Fluorescein isothiocyanate (FITC)-conjµgated mAbs to HLA-DR (L243), Phycoerythrin (PE)-

conjµgated mAbs to CD80 (2D10), CD69 (FN50), IFN-γ (4S.B3), allophycocyanin (APC)-conjµgated mAbs to FOXP-3 (236A/E7), IL-2 (MQ1-17H12), and CD68 (Y1/82A), PerCP-conjµgaed mAbs to CD8 (HIT8a), and CD16 (3G8), APC-Cy7-conjµgated anti HLA-A,B,C (W6/32), BV421-conjµgated anti CD14 (HCD14), and TNF-α (MAb11), PE-Cy7-conjµgated anti CD11b (ICRF44), CD3 (HIT3a), Alexa-Fluor 700-conjugated mAbs to CD11c (3.9), and CD40 (5C3), PE-CF594-conjugated mAbs to CD86 (2331), and CD4, BV605-conjugated Ep-CAM (9C4), and BV-785-conjugated mAb to CD45 (HI30) were purchased from BD Biosciences (San Jose, CA), Biolegend (San Diego, CA), or eBioscience (Santa Clara, CA). Fixable aqua viability dye was purchased from Invitrogen (Carlsbad, CA).

The following antibodies were utilized for staining in FACS analyses and/or cell sorting in mouse studies: FITC/AF488-conjµgated mAbs to Ly6C (HK1.4), CD49b(DX5), CD244.2(2B4), KLRG1(2F1), CD45(30-F11), H2(M1/42), CD45(30-F11), CD95(15A7), Rat IgG(eBRG1), PE-conjµgated mAbs to B7-DC(122), CD19(6D5), CTLA-4(UC10-4B9), CD44(1M7), ARP(YGIC86), CD47(miap301), Rat IgG(eBio299Arm), PerCP-conjµgaed mAbs to Ly6G(1A8), Nkp46(29A1.4), Foxp3(FJK-16s), CD45(30-F11), H2d(AF6-88.5), EpCAM(G8.8), Rat IgG(eBRG1), APC/AF647-conjµgated mAbs to F4/80(BM8), CD160(7H1), TIM3(B8.2C12), BTLA(6A6), Epcam(G8.8), PD-L1(10F.9G2), Foxp3(FJK-16s), Rat IgG(eBR2a), Ef450/Pacific Blue/BV421-conjugated mAbs to CD86(GL1), CD11a(M1714), LAG-3(eBioC9B7W), Ki67(16A8), CCR4(2G12), F4/80(BM8), CD4(RM4-5), Rat IgG(eBRG1), PE-Cy7-conjµgated mAbs to CD11b(M1/70), CD3(17A2), PD1(RMP1-30), CD62L(MEL-14), PD-L1(10F.9G2), CD69(H1.2F3), Rat IgG(RTK2758), APC-Cy7-conjµgated mAbs to CD11c(N418), CD4(GK1.5), CD45(30-F11), Alexa-Fluor 700-conjugated mAbs to IA/IE(M5/114.15.2), CD8(53-6.7), Rat IgG(RTK4530), were purchased from BD Biosciences

(San Jose, CA), Biolegend (San Diego, CA), or eBioscience (Santa Clara, CA). Anti-alpha tubulin (acetyl K40) antibody (EPR16772) and goat anti-rabbit IgG H&L FITC were purchased from abcam (Cambridge, MA). Phospho-STAT5 alpha (Tyr694) antibody was purchased from Invitrogen (Rockford, Illinois).

In vivo antibodies anti-CD4 (GK1.5), anti-CD8 (53-6.72), and rat IgG (LTF-2) were purchased from Bio X Cell (Lebanon, NH). Mice were first administered two consecutive doses (400μg/mouse) of antibodies at day -2 and day -1 and twice per week thereafter along with ricolinostat and JQ1 combination treatment.

Flow Cytometry

Staining for alpha tubulin (acetyl K40) was performed according to manufacturer's instructions. Briefly, tumor cell suspensions were stained for CD45,CD3, CD4, CD11c, and CD11b after which cells were fixed with 2% paraformaldehyde prior to labelling with purifiedanti-alpha tubulin antibody for 1 hour. Cells were subsequently incubated for 30 mins with goat anti-rabbit IgG FITC secondary antibody. For evaluation of Phospho-STAT5 alpha, cell suspensions stained for surface antigens as above were fixed with ebioscience Foxp3 fixation buffer after which cells were incubated with 5% BSA for 1 hour. Cells were then labelled with unconjugaed anti-Phospho STAT5 alpha (Tyr694) primary antibody for 1 hour followed by 30-minute incubation with FITC-conjugated goat anti-rabbit secondary antibody.

Mass cytometry (CyTOF)

The following antibodies were used for CyTOF analyses: 154Sm-conjugated mAbs to CD45 (HI30), 170Er-conjugated mAbs to CD3 (UCHT1), 174Yb-conjugated mAbs to CD4 (SK3),

168Er-conjugated mAbs to CD8 (SK1), 149Sm-conjugated mAbs to CD25 (2A3), 169Tm-conjugated mAbs to CD45RA (HI100), 162Dy-conjugated mAbs to CD69 (FN50), and 158Gd-conjugated mAbs to pStat3 [Y705] (4/P-Stat3) were purchased from Fluidigm. 165Ho-conjugated mAbs to Foxp3 (PCH101) was conjugated using a purified antibody (eBioscience) with the MaxPar X8 antibody labeling kit (Fluidigm). 173Yb-conjugated mAbs to CCR7 (G043H7) was conjugated using a purified antibody (Biolegend) with the MaxPar DN3 antibody labeling kit (Fluidigm). Procedures for mass cytometry antibody staining were carried out according to the manufacturer's protocol (Fluidigm). The mass cytometry data were acquired by CyTOF-2 mass cytometer (Fluidigm). Two-dimensional gating analysis was conducted using Cytobank. Visualization of high dimensional mass cytometry data was done using viSNE map.

Single cell RNA sequencing of tumor-infiltrating TAMs and T cells

Briefly, total RNA was purified from sorted cells using RNA-SPRI beads. Poly(A)+ mRNA was converted to cDNA which was then amplified. cDNA was subject to transposon-based fragmentation that used dual-indexing to barcode each fragment of each converted transcript with a combination of barcodes specific to each sample. In the case of single cell sequencing, each cell was given its own combination of barcodes. Barcoded cDNA fragments were then pooled prior to sequencing. Sequencing was carried out as paired-end 2x25bp with an additional 8 cycles for each index. The Smart-Seq2 data was processed at the Broad Technology Labs according to established computational pipeline. Data was separated by barcode and aligned using Tophat version 2.0.10 (Kim et al., 2013) with default settings. Paired-end (PE) 25bp reads were mapped to the UCSC human genome (hg19) by Bowtie2/Tophat (Trapnell et al., 2009) using the Broad pipeline. Only cells that had a minimum of 100,000 PE reads, and with at least

20% aligning to the genome, were retained for further analysis. FeatureCounts (Liao et al., 2014) was used to count features based on the Gencode v19 (http://www.gencodegenes.org/) transcriptome annotation. Features that were not detected in more than 10 cells were removed. High quality single-cells were further selected based on feature complexity, read distribution, and number of genes detected. In total 9 normal and 55 tumor cells were retained in this process. DESeq2 (Love et al., 2014) was used to detect differentially expressed genes between groups based on raw counts. Counts were normalized according to their library size and displayed as log2 (normalized counts + 1).

Nanostring array analysis of Tumor-infiltrating TAMs and T cells

Gene transcript levels were assessed by nanostring as previously described (ref). For each sample, mRNA transcript abundance for ~780 genes of interest was quantified using the Nanostring nCounter Mouse PanCancer Immune Profiling Panel according to the manufacturer's protocol from 100 ng of total RNA and analyzed using nSolver 2 software and the HumanPanCancerImmunology_1.0.36 analysis module.

Differential expression of genes in response to ricolinostat or JQ1 treatment relative to vehicle was performed in the advanced Analysis module of nSolver. For each gene, a single linear regression was fit using all selected covariates to predict expression. Output is shown with nonadjusted *P* value as well as Benjamini- Hochberg FDR.